Experimental and theoretical cross sections for electron-impact excitation of the $2s \rightarrow 2p$ transition in O^{5+}

J. A. Lozano,[1] M. Niimura,[2] S. J. Smith,[2] A. Chutjian,[2] and S. S. Tayal[3]
[1]*Physics Department, University of Connecticut, Storrs, Connecticut 06269*
[2]*Jet Propulsion Laboratory, California Institute of Technology, Pasadena, California 91109*
[3]*Physics Department, Clark Atlanta University, Atlanta, Georgia 30314*
(Received 2 October 2000; published 20 March 2001)

Experimental and *R*-matrix calculated cross sections are reported for the resonance $2s \rightarrow 2p$ transition in O^{5+}. Use is made in the measurements of the electron-energy-loss technique, with center-of-mass interaction energies in the range 10.5 (below threshold) through 12.0 (threshold) to 17.0 eV. The present results are in good agreement with calculations using the *R* matrix with pseudostates theory, which includes nine physical states and 18 pseudostates. They are also in good agreement with near-threshold data of Bell *et al.* [Phys. Rev. A **49**, 4585 (1994)], and with a 41-state calculation of Griffin *et al.* [J. Phys. B **33**, 1013 (2000)].

DOI: 10.1103/PhysRevA.63.042713 PACS number(s): 34.80.Kw

I. INTRODUCTION

The excitation of highly charged ions (HCIs) by electrons is a process responsible for visible, UV, and x-ray emissions observed in astrophysical plasmas and magnetically confined fusion plasmas. In stellar spectra transitions in O^{5+} have been observed by the Extreme Ultraviolet Explorer (EUVE) [1] and the Far Ultraviolet Spectroscopic Explorer (FUSE) satellites [2]; in white dwarfs by the Orbiting and Retrievable Far and Extreme Ultraviolet Spectrometers (ORFEUS) [3]; and in the solar corona by the Solar and Heliospheric Observatory (SOHO) [4]. In fact, the O^{5+} $2s \rightarrow 2p$ resonance doublets are two of the brightest emitters in the upper solar transition region [5]. Closer to home, a multitude of highly charged ions, including O^{5+}, partake of electron cooling and radiative loss in stellarlike laboratory fusion plasmas [6,7].

Presented here are measurements of absolute electron-impact excitation cross sections for the O^{5+} combined (unresolved) doublet resonance transitions $^2S_{1/2} \rightarrow {}^2P^o_{1/2,3/2}$. These measurements are in good agreement with earlier results near threshold [8] using the energy-loss method, and provide data at higher energies for comparison with theory. The present calculations use the multistate *R*-matrix method including nine physical states and 18 pseudostates of the e-O^{5+} system. An experimental summary is given in Sec. II, details of the theoretical approach in Sec. III, and results of the present experiment and theory in Sec. IV, with comparison to other experiments and theory.

II. EXPERIMENT

The experimental techniques used in the present measurements were similar to those used in Greenwood *et al.* [9]. Briefly, a beam of O^{5+} ions is extracted from an electron-cyclotron resonance ion source (ECRIS), momentum-analyzed, and focused into the collision region. A magnetically-confined beam of low-energy electrons is scattered from the electrostatically-focused O^{5+} beam in a merged electron-ion beams geometry. After the collisions, the electrons are velocity analyzed in a trochoidal monochromator (TM), and detected by means of a position-sensitive detector (PSD) at the output plane of the TM. Absolute cross sections are obtained for data near threshold, where the elastically-scattered (Rutherford) electrons are well separated from the inelastically-scattered events. At energies sufficiently above threshold, some portion of the elastic events overlap the inelastic events, where axial electron velocities can be close to one another. Baseline subtractions of 0% (near threshold) to 25% (at the highest energy), derived from calculated elastic electron-ion cross sections, are applied to these data to eliminate the elastic contribution. Details are given in Ref. [9], and references therein.

The basic equation relating the laboratory-measured quantities, or those quantities whose values are nominally known (the electron and ion velocities), is given by

$$\sigma(E) = \frac{\mathbb{R} q e^2 \mathcal{F}}{\epsilon I_i I_e L} \left| \frac{v_e v_i}{v_e - v_i} \right|. \tag{1}$$

Here, $\mathbb{R}$ is the net signal rate (s^{-1}), q is the ion charge state (C), e is the unit of electron charge (C), $\mathcal{F}$ is the spatial overlap factor between the electron and ion beams (cm^2), v_e and v_i are the electron and ion velocities ($cm\,s^{-1}$), ϵ is the efficiency of the combined rejection-grids–microchannel-plate detection system (dimensionless), I_e and I_i are the electron and ion currents, respectively ($C\,s^{-1}$), and L is the merged path length (cm).

As in earlier work, the fraction f of the incident ion beam in a metastable state(s) must be assessed. Ions in metastable levels are unavailable for excitation of the ground-state $2s \rightarrow 2p$ transition, and hence the ion current I_i to be used in Eq. (1) is only a fraction $(1-f)$ of the current measured at the Faraday cup. Therefore all cross sections must be increased by the factor $(1-f)^{-1}$. In the case of lithiumlike O^{5+} the first singlet and triplet metastable levels are high lying, at 56.9 and 56.1 eV, respectively. It is often argued that such high-lying levels would not be expected to have significant population in the ECR plasma. Nevertheless, this

TABLE I. Calculated and experimental energies (in Ry) for O^{5+}.

State	Calculated energy (present work)	Experimental energy
$1s^2 2s\ ^2S$	0.000 00	0.000 00
$1s^2 2p\ ^2P^o$	0.895 11	0.881 47
$1s^2 3s\ ^2S$	5.829 43	5.832 47
$1s^2 3p\ ^2P^o$	6.069 57	6.071 03
$1s^2 3d\ ^2D$	6.142 45	6.147 92
$1s^2 4s\ ^2S$	7.767 57	7.770 34
$1s^2 4p\ ^2P^o$	7.863 23	7.867 66
$1s^2 4d\ ^2D$	7.893 54	7.899 71
$1s^2 4f\ ^2P^o$	7.894 82	7.901 44

population was measured in the present work by use of the beam-attenuation method, and was found to be negligible to within a 2% error.

III. THEORETICAL DETAILS

Cross sections for electron-impact excitation of the resonance $2s \rightarrow 2p$ transition in O^{5+} were calculated using the *R* matrix with pseudostates (RMPS) approach. Included in the close-coupling expansions were the nine physical states $2s$, $2p$, $3s$, $3p$, $3d$, $4s$, $4p$, $4d$, and $4f$ together with 18 pseudostates $\overline{5s}-\overline{9s}$, $\overline{5p}-\overline{9p}$, $\overline{5d}-\overline{8d}$, and $\overline{5f}-\overline{8f}$. The physical states as well as pseudostates are represented by configuration-interaction (CI) expansions. The $1s$ and $2s$ orbitals are taken from [10] and the other physical orbitals $2p$, $3s$, $3p$, $3d$, $4s$, $4p$, $4d$, and $4f$ are obtained by the use of structure code CIV3 [11] through minimization of energies of the respective O^{5+} target states. The pseudo-orbitals $\overline{5s}-\overline{9s}$, $\overline{5p}-\overline{9p}$, $\overline{5d}-\overline{8d}$, and $\overline{5f}-\overline{8f}$ are constructed as linear combinations of Sturmian-type functions $r^n \exp(-\alpha r)$ with the range parameter $\alpha = 1.70$ for $\overline{5s}-\overline{9s}$ and $\overline{5d}-\overline{8d}$ orbitals, 1.75 for $\overline{5p}-\overline{9p}$ orbitals, and 1.80 for $\overline{5f}-\overline{8f}$ orbitals. With these range parameters all orbitals are contained in an *R*-matrix box of radius $a = 11.8$ a.u.

The pseudo-orbitals are orthogonal to each other and to physical orbitals with the same orbital angular momentum. The calculated excitation energies of the physical target states relative to the ground $2s\ ^2S$ state are given in Table I, and are compared with measured values [12]. The present excitation energies are within 1% of experimental results except for the $2p\ ^2P^o$ state where they differ by about 1.5%. We also calculated length and velocity values of the oscillator strength for the dipole-allowed transitions. These are listed in Table II and compared with the NIST compilation [13]. Good agreement is found between the length and velocity values of oscillator strength, and with the best available values from the NIST compilation.

The one-body mass correction and Darwin relativistic terms, which do not give rise to fine-structure splitting, are included in the scattering equations in the Breit-Pauli approximation [14]. The total wave function representing scattering of electrons from O^{5+} ion for each angular momentum

TABLE II. Oscillator strengths of dipole-allowed transitions in O^{5+}.

	Calculated *f* values (present work)		NIST (Ref. [13])
Transition	f_L	f_V	
$2s$-$2p$	0.202	0.236	0.199
$2s$-$3p$	0.265	0.262	0.265
$2s$-$4p$	0.074	0.073	0.074
$2p$-$3s$	0.029	0.031	0.029
$2p$-$4s$	0.006	0.006	0.006
$2p$-$3d$	0.660	0.660	0.657
$2p$-$4d$	0.124	0.122	0.123
$3p$-$4s$	0.065	0.064	0.064
$3p$-$3d$	0.045	0.054	0.049
$3p$-$4d$	0.562	0.555	0.557
$3d$-$4p$	0.015	0.015	0.015
$4s$-$4p$	0.454	0.478	0.462
$4p$-$4d$	0.080	0.085	0.086
$3d$-$4f$	1.016	1.016	1.020
$4d$-$4f$	0.0016	0.0018	0.0024

L, spin *S*, and parity π is expanded in the inner region ($r \leqslant a$) in the *R*-matrix basis [15]. The diagonal elements of the inner-region ($r < a$) Hamiltonian matrix are adjusted to reproduce observed energies of physical target states in our scattering calculation.

We included 25 continuum orbitals for each angular momentum. The coupled equations are solved in the outer region using a perturbation method to yield *K* matrices and then cross sections. The *R*-matrix method is used to calculate cross sections for partial waves with angular momentum $L = 0-57$. These partial waves are sufficient to give a converged cross section of the $2s \rightarrow 2p$ transition in the energy region from threshold to 20 eV. The present results are in good agreement with the recent RMPS calculation of Griffin, Badnell, and Pindzola [16].

IV. EXPERIMENTAL AND CALCULATED RESULTS

Experimental and theoretical results are shown in Fig. 1 as a function of collision energy, and all results are presented in Table III. The error bars in Fig. 1 are given at the 1.7σ or 90% confidence level, and are absolute errors for each data point. Details of the individual contributing uncertainties are the same as given in Table I of Ref. [17]. The energy spread in the present measurements is approximately 125 meV [full width at half maximum (FWHM)] as measured by the retarding-potential method on the incident electron beam. Additional measurements are available in the threshold region from Ref. [8]. Use here was also made of the energy-loss, merged-beam technique, with differences: some in geometry [e.g., the merged-beam length, method of measuring the form factor $\mathcal{F}$ in Eq. (1), and placement of the PSD in the electron analyzer] and some in the scattering diagnostics (use herein of an electron mirror and electronic aperture). The present experimental results are given as solid circles, and

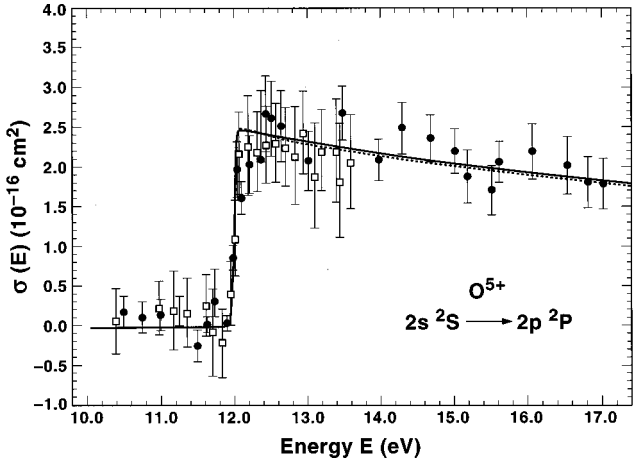

FIG. 1. Experimental cross sections vs center-of-mass energy for excitation of the $2s\ ^2S_{1/2} \rightarrow 2p\ ^2P^o_{1/2,3/2}$ transitions in O^{5+}. The present energy-loss results are given as filled circles, with absolute error bars shown at the 90% confidence level (1.7σ). Other results are energy-loss measurements near threshold (open squares, with mainly relative error bars [8]). The solid line represents results of the present *R* matrix with pseudostates calculation using nine physical states and 18 pseudostates; the dashed line represents results of the 41-state RMPS calculation of Ref. [16].

earlier measurements [8] by open squares. Very good agreement is evident between the two sets of measurements in the overlapping energy region. The present data extend the measurements [8] from 13.6 to 17.0 eV. This was possible by combined use of retarding grids and the electronic aperture to reject higher-energy elastically scattered electrons; and a systematic fields-and-trajectories modeling and background subtraction consistent with the theoretically expected transmission of the remaining elastically scattered electrons having the same axial velocity as the inelastically scattered electrons. Using this combined analysis one does not find any significant or unexplained scattering [8] from sources other than inelastic scattering, either below or above threshold.

Also shown in Fig. 1 (solid curve) are results of the present RMPS approach. There is excellent agreement between experiment and theory over the entire energy range. Cross sections were calculated at a fine energy mesh (0.0136 eV). As in the case of the C^{3+} $2s$-$2p$ dipole transition, there is no evidence of resonance structure in this energy range (within the present energy resolution) owing to the dominance of the longer-range dipole scattering over the shorter-range resonance interaction. The theoretical 41-state RMPS cross sections of Ref. [16] are also shown for comparison in Fig. 1. These results are similarly smooth in the energy region from threshold to 30 eV. The peak value of the 41-state cross section is about 0.5% higher than that of the present calculation, and results lie about 0.05% lower at higher energies. Griffin *et al.* [16] note that the inclusion of $n=5$ physical states and pseudostates in the close-coupling expansion has insignificant effect on the cross sections for the $2s$-$2p$ transition. Both theoretical results agree well with the experiments, to within uncertainties.

In conclusion, experimental and theoretical cross sections for electron-impact excitation of the resonance $2s$-$2p$ transition in O^{5+} are presented from threshold to 17.5 eV. There is excellent agreement between the present experiment and theory, and with one other measurement and calculation.

TABLE III. Absolute cross sections for electron-impact excitation of the $2s\ ^2S \rightarrow 2p\ ^2P$ transition in O^{5+}. Also listed are experimental collision strengths (last column) for convenience in plasma-modeling applications.

Energy[a] (ev)	Energy[a] (Ry)	Cross section[b] (10^{-16} cm^2)	Collision strength Ω(E) (dimensionless)
10.5	0.7717	0.170[c]	0.298
10.7_5	0.7901	0.100	0.180
11.0	0.8085	0.130	0.239
11.5	0.8452	−0.260	−0.500
11.6	0.8526	0.010	0.019
11.7	0.8599	0.300	0.586
11.9	0.8746	0.024	0.048
11.9_3	0.8805	0.853	1.71
12.0_3	0.8842	1.96	3.94
12.1	0.8893	1.60	3.23
12.2	0.8967	2.02	4.12
12.3_6	0.9084	2.08	4.30
12.4_2	0.9129	2.66	5.52
12.5	0.9187	2.60	5.43
12.6	0.9283	2.50	5.26
13.0	0.9555	2.07	4.50
13.5	0.9922	2.67	6.02
14.0	1.0290	2.08	4.87
14.3	1.0510	2.48	5.93
14.7	1.0804	2.35	5.77
15.0	1.1025	2.16	5.41
15.2	1.1172	1.87	4.75
15.5	1.1392	1.70	4.40
15.6	1.1466	2.05	5.34
16.0	1.1760	2.19	5.85
16.5	1.2127	2.01	5.54
16.8	1.2348	1.80	5.05
17.0	1.2495	1.78	5.06

[a]The electron-energy scale is accurate to ±0.05 eV.
[b]Experimental errors are 18% at the 1.7σ or 90% confidence level.
[c]Nonzero values below threshold include effects of the electron-energy spread (approx. 0.125 eV) and statistical errors in the measurement of the cross section.

ACKNOWLEDGMENTS

J.A.L. thanks the University of Connecticut NASA/EPSCOR program for support while at JPL; M.N. acknowledges support by the NASA-NRC program; and S.S.T. acknowledges support by the NASA Planetary Atmospheres Program. We thank D. Griffin for providing numerical results of the 41-state RMPS calculation. The present computational work was carried out on the JPL/Caltech Cray Supercomputer. The experimental work was carried out at JPL/Caltech through agreement with NASA.

[1] A. K. Dupree, N. S. Brickhouse, G. A. Doschek, J. C. Green, and J. C. Raymond, Astrophys. J. **418**, L41 (1993).
[2] A. W. Fullerton, P. A. Crowther, O. DeMarco, J. B. Hutchings, L. Bianchi, K. R. Brownberger, D. L. Massa, D. C. Morton, B. L. Rachford, T. P. Snow, G. Sonneborn, J. Tulinson, and A. J. Willis, Astrophys. J. Lett. **538**, L43 (2000).
[3] J. C. Raymond, C. W. Mauche, S. Bowyer, and M. Hurwitz, Astrophys. J. **440**, 331 (1995).
[4] U. Feldman, W. E. Behring, W. Curdt, U. Schühle, K. Wilhelm, P. Lemaire, and T. M. Moran, Astrophys. J., Suppl. Ser. **113**, 195 (1997).
[5] W. Curdt, U. Feldman, J. M. Laming, K. Wilhelm, U. Schühle, and P. Lemaire, Astron. Astrophys. Suppl. Ser. **126**, 281 (1997).
[6] G. H. Dunn, Nucl. Fusion Suppl. S **2**, 25 (1992).
[7] X. Bonin, R. Marchand, and R. K. Janev, Nucl. Fusion Suppl. S **2**, 117 (1992).
[8] E. W. Bell, X. Q. Guo, J. L. Forand, K. Rinn, D. R. Swenson, J. S. Thompson, G. H. Dunn, M. E. Bannister, D. C. Gregory, R. A. Phaneuf, A. C. H. Smith, A. Müller, C. A. Timmer, E. K. Wåhlin, B. D. DePaola, and D. S. Belić, Phys. Rev. A **49**, 4585 (1994).
[9] J. B. Greenwood, S. J. Smith, A. Chutjian, and E. Pollack, Phys. Rev. A **59**, 1348 (1999).
[10] E. Clementi and C. Roetti, At. Data Nucl. Data Tables **14**, 177 (1974).
[11] A. Hibbert, Comput. Phys. Commun. **9**, 141 (1975).
[12] C. E. Moore, *Atomic Energy Levels*, Nat. Bur. Stand. (U.S.) Circ. No. 467 (U.S. GPO, Washington, DC, 1949), Vol. I.
[13] W. L. Wiese, J. R. Fuhr, and T. M. Deters, J. Phys. Chem. Ref. Data Monogr. No. 7 (1996).
[14] N. S. Scott and P. G. Burke, J. Phys. B **13**, 4299 (1980).
[15] K. A. Berrington, W. B. Eissner, and P. H. Norrington, Comput. Phys. Commun. **92**, 290 (1995).
[16] D. C. Griffin, N. R. Badnell, and M. S. Pindzola, J. Phys. B **33**, 1013 (2000).
[17] S. J. Smith, M. Zuo, A. Chutjian, S. S. Tayal, and I. D. Williams, Astrophys. J. **463**, 808 (1996).